Inorganic Chemistry
Article

Inorg. Chem. **2010**, *49*, 2427–2434 **2427**
DOI: 10.1021/ic902360x

Discrete Tetrairon(III) Cluster Exhibiting a Square-Planar $Fe_4(\mu_4\text{-}O)$ Core: Structural and Magnetic Properties

Mariappan Murali,[†,‡] Sanjit Nayak,[†] José Sánchez Costa,[§] Joan Ribas,[§] Ilpo Mutikainen,[∥] Urho Turpeinen,[∥] Martin Clémancey,[⊥] Ricardo Garcia-Serres,[⊥] Jean-Marc Latour,[⊥] Patrick Gamez,*[,†] Geneviève Blondin,*[,⊥] and Jan Reedijk[†]

[†]*Leiden Institute of Chemistry, Gorlaeus Laboratories, Leiden University, P.O. Box 9502, 2300 RA Leiden, The Netherlands,* [§]*Departament de Química Inorgànica, Universitat de Barcelona, Diagonal 647, 08028 Barcelona, Spain,* [∥]*University of Helsinki, Department of Chemistry, Laboratory of Inorganic Chemistry, FIN-00014 Helsinki, Finland, and* [⊥]*Laboratoire de Chimie et Biologie des Métaux, Université Joseph Fourier, CNRS UMR 5249, CEA, DSV/iRTSV, 17 rue des Martyrs, 38054 Grenoble cedex 9, France.* [‡]*On leave from Department of Chemistry, National College, Tiruchirappalli 620 001 Tamil Nadu, India*

Received November 29, 2009

The aerobic reaction of the Schiff-base ligand *N*-(benzimidazol-2-yl)salicylaldimine (**Hbisi**) with iron(II) perchlorate in methanol leads to the formation of the remarkable coordination compound $[Fe_4(\mu_4\text{-}O)(\mu\text{-}MeO)_4(bisi)_4](ClO_4)_2\cdot 4MeOH$ (**1**), whose single-crystal X-ray structure reveals the presence of a discrete $Fe^{III}{}_4(\mu_4\text{-}O)$ core. Magnetic and Mössbauer studies both show that the exchange interaction within the square tetranuclear iron(III) unit is dominated by the central bridging μ_4-oxido ligand, the involvement of the μ-methoxido bridges being negligible.

Introduction

The design and preparation of polynuclear oxido-, hydroxido-, and alkoxido-bridged iron clusters have received considerable interest during the past 20 years,[1−6] mainly for two reasons. First, such coordination compounds may represent biomimetic models[7−10] for the iron oxide/hydroxide core of the iron storage protein ferritin, that can accommodate up to 4500 iron ions,[11−13] as well as other biological systems.[14,15] Second, high-nuclearity iron compounds with high-spin ground states and large negative magnetic anisotropy can exhibit single-molecule magnet (SMM) behavior.[16−19]

Constant research efforts are dedicated to the search for new synthetic methods that may generate original polynuclear Fe/O clusters with interesting properties.[20] In that context, a very efficient synthetic strategy to prepare high-nuclearity Fe_n ($n > 3$) clusters consists in reacting organic ligands (very often alcohol-based chelate ligands)[21] with trinuclear coordination compounds containing the triangular, oxide-centered $[Fe_3(\mu_3\text{-}O)]^{7+}$ core.[22,23]

*To whom correspondence should be addressed. E-mail: p.gamez@chem.leidenuniv.nl (P.G.), genevieve.blondin@cea.fr (G.B.).

(1) Que, L.; True, A. E. *Prog. Inorg. Chem.* **1990**, *38*, 97–200.
(2) Schneppensieper, T.; Liehr, G.; van Eldik, R.; Ensling, J.; Gutlich, P. *Inorg. Chem.* **2000**, *39*, 5565–5568.
(3) Glaser, T.; Lugger, T.; Hoffmann, R. D. *Eur. J. Inorg. Chem.* **2004**, 2356–2362 and references therein.
(4) Islam, Q. T.; Sayers, D. E.; Gorun, S. M.; Theil, E. C. *J. Inorg. Biochem.* **1989**, *36*, 51–62.
(5) Aromi, G.; Brechin, E. K. *Struct. Bonding* (*Berlin*) **2006**, *122*, 1–67.
(6) Gatteschi, D.; Caneschi, A.; Sessoli, R.; Cornia, A. *Chem. Soc. Rev.* **1996**, *25*, 101–109.
(7) Nair, V. S.; Hagen, K. S. *Inorg. Chem.* **1992**, *31*, 4048–4050.
(8) Taft, K. L.; Papaefthymiou, G. C.; Lippard, S. J. *Inorg. Chem.* **1994**, *33*, 1510–1520.
(9) Taft, K. L.; Papaefthymiou, G. C.; Lippard, S. J. *Science* **1993**, *259*, 1302–1305.
(10) Nesterova, M. V.; Walton, S. A.; Webb, J. *J. Inorg. Biochem.* **2000**, *79*, 109–118.
(11) Theil, E. C.; Matzapetakis, M.; Liu, X. F. *J. Biol. Inorg. Chem.* **2006**, *11*, 803–810.
(12) Powell, A. K. *Struct. Bonding* (*Berlin*) **1997**, *88*, 1–38.
(13) Proulx-Curry, P. M.; Chasteen, N. D. *Coord. Chem. Rev.* **1995**, *144*, 347–368.
(14) Wallar, B. J.; Lipscomb, J. D. *Chem. Rev.* **1996**, *96*, 2625–2657.
(15) Lippard, S. J. *Angew. Chem., Int. Ed.* **1988**, *27*, 344–361.
(16) Taguchi, T.; Stamatatos, T. C.; Abboud, K. A.; Jones, C. M.; Poole, K. M.; O'Brien, T. A.; Christou, G. *Inorg. Chem.* **2008**, *47*, 4095–4108.
(17) Boudalis, A. K.; Lalioti, N.; Spyroulias, G. A.; Raptopoulou, C. P.; Terzis, A.; Bousseksou, A.; Tangoulis, V.; Tuchagues, J. P.; Perlepes, S. P. *Inorg. Chem.* **2002**, *41*, 6474–6487.
(18) Barra, A. L.; Caneschi, A.; Cornia, A.; de Biani, F. F.; Gatteschi, D.; Sangregorio, C.; Sessoli, R.; Sorace, L. *J. Am. Chem. Soc.* **1999**, *121*, 5302–5310.
(19) Oshio, H.; Hoshino, N.; Ito, T. *J. Am. Chem. Soc.* **2000**, *122*, 12602–12603.
(20) Gatteschi, D.; Caneschi, A.; Pardi, L.; Sessoli, R. *Science* **1994**, *265*, 1054–1058.
(21) Murugesu, M.; Abboud, K. A.; Christou, G. *Polyhedron* **2004**, *23*, 2779–2788.
(22) Murugesu, M.; Abboud, K. A.; Christou, G. *Dalton Trans.* **2003**, 4552–4556.
(23) Brechin, E. K.; Knapp, M. J.; Huffman, J. C.; Hendrickson, D. N.; Christou, G. *Inorg. Chim. Acta* **2000**, *297*, 389–399.

Published on Web 02/02/2010

Thus, a number of coordination compounds where iron ions are bridged by a μ_n-oxido ligand (n = 1 to 6) have been described in the literature. Thus, the $Fe_2(\mu\text{-O})$,[24,25] $Fe_3(\mu_3\text{-O})$,[26,27] $Fe_4(\mu_4\text{-O})$,[28,29] $Fe_5(\mu_5\text{-O})$,[30,31] and $Fe_6(\mu_6\text{-O})$[32,33] motifs have been observed in the solid-state structures of iron coordination compounds.

In the course of our investigations aimed at preparing polynuclear metal complexes with attractive magnetic properties, the new Schiff-base ligand *N*-(benzimidazol-2-yl)-salicylaldimine (**Hbisi**; Scheme 1) has been prepared. The aerobic reaction of iron(II) perchlorate with the ligand **Hbisi** in methanol produces the compound $[Fe_4(\mu_4\text{-O})(\mu\text{-MeO})_4(\mathbf{bisi})_4](ClO_4)_2\cdot 4MeOH$ (**1**), whose single-crystal X-ray structure reveals a $Fe^{III}_4(\mu_4\text{-O})$ unit. Such discrete $Fe_4(\mu_4\text{-O})$ units are extremely rare; actually, $[Fe^{II}_4(\mu_4\text{-O})]^{6+}$ cores have been observed, with various geometries, only in three coordination compounds, namely, $[Fe_4O(dpa)_6]\cdot 2$toluene (dpa = anion of the dipyridylamine; CSD refcode XIRFIN),[34] $[Fe_4O(DPhF)_6]\cdot 1.5$toluene (DPhF = *N*,*N*′-diphenylformamidinate; CSD refcode NEKXOQ),[35] and $[Fe_4O(MBT)_6]$ (MBT = 2-mercaptobenzothiazole; CSD refcode HEQVAB).[36] To the best of our knowledge, a *discrete*, square-planar $[Fe^{III}_4(\mu_4\text{-O})]^{10+}$ core has never been reported so far. In fact, this iron(III) motif has only been found as part of higher-nuclearity clusters.[37,38] This prompted us to study the electronic structure of compound **1** through magnetic susceptibility measurements and Mössbauer spectroscopy.

Experimental Section

Materials and Methods. Solvents and chemicals were commercially available as A.R. grade and used as received. All reactions and purifications were performed in air. Proton magnetic resonance (^{1}H NMR) spectra were recorded on a DPX 300 Bruker (300 MHz) spectrometer at 25 °C. Proton chemical shifts are expressed in parts per million (ppm, δ scale) and are referenced to the solvent peak. Infrared spectra were recorded using a Perkin-Elmer Paragon 1000 spectrophotometer equipped with a Golden Gate Diamond ATR as a sample support, and data are represented as the frequency of absorption

Scheme 1. Ligand *N*-(benzimidazol-2-yl)salicylaldimine (**Hbisi**)

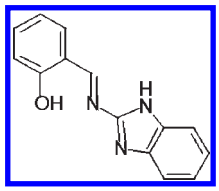

(cm^{-1}). C, H, N analyses were carried out using an automatic Perkin-Elmer 2400 Series II CHNS/O analyzer. ESI Mass Spectroscopy was carried out using a Finnigan AQA Mass Spectrometer equipped with an electrospray ionization (ESI) source. Sample solutions (10 μL of a 1 mg mL^{-1} solution) were introduced in the ESI source by using a Dionex ASI-100 automated sampler injector and an eluent running at 0.2 mL·min^{-1}. Variable temperature and field magnetic measurements were performed on a polycrystalline sample of **1**, in the range 2−300 K using a Quantum Design MPMS-7XL SQUID magnetometer in fields of 0−7 T. Corrections for the diamagnetic contribution of the complex, deduced from Pascal's tables,[39] and for the sample holder were applied. ^{57}Fe Mössbauer spectra have been recorded at 4.2 K, 25, 35, and 50 K on a strong-field Mössbauer spectrometer equipped with an Oxford Instruments Spectromag 4000 cryostat containing an 8 T split-pair superconducting magnet. The spectrometer was operated in a constant acceleration mode in transmission geometry. The isomer shifts are referenced against that of a room-temperature metallic iron foil. The analysis of the data was performed with the software package WMOSS (WEB Research, Edina, MN, www.wmoss.org).

Synthesis of *N*-(benzimidazol-2-yl)salicylaldimine (Hbisi). A solution of salicylaldehyde (3.1 g, 0.025 mol) in methanol (10 mL) was added, under constant stirring, to a solution of 2-aminobenzimidazole (3.3 g, 0.025 mol) in methanol (30 mL). The reaction mixture was refluxed (70 °C) for 2 h. The methanol was evaporated to dryness under reduced pressure to yield a yellow solid. The solid material was redissolved in hot methanol (25 mL) and left at room temperature for 1 day. Bright-yellow crystals were then collected from the mixture, washed three times with CH_2Cl_2 (25 mL), and dried in vacuum. Yield: 5.3 g, 89%; ^{1}H NMR (DMSO-d_6, 300 MHz): δ 7.02 (d, 1H), 7.58 (t, 1H), 7.01 (t, 1H), 7.86 (d, 1H), 12.75 (s, 1H, −OH), 7.47 (m, 2H), 7.19 (m, 2H), 12.09 (s, 1H, −NH−) and 9.65 (s, 1H, −CH=N−) ppm. IR (neat): 3370, 2990, 1652, 1622, 1612, 1558, 1532, 1481, 1428, 1340, 1313, 1271, 1199, 1147, 1107, 1050, 1003, 993, 917, 898, 854, 789, 758, 739, 668, 614, 585, 556 cm^{-1}. ESI-MS: 238 $(M+H)^+$. Elemental analyses, found (calcd. for $C_{14}H_{11}N_3O$): C, 70.46 (70.87); H, 4.66 (4.67); N, 17.71 (17.71).

Synthesis of $[Fe_4(\mu_4\text{-O})(\mu\text{-MeO})_4(bisi)_4](ClO_4)_2\cdot 4MeOH$ (1). A methanolic solution (10 mL) of the ligand **Hbisi** (119 mg; 0.5 mmol) was prepared. An equimolar methanolic solution (10 mL) of $Fe^{II}(ClO_4)_2\cdot 6H_2O$ (181 mg; 0.5 mmol) was added to the ligand solution. The resulting dark solution was stirred for 10 min at room temperature and then filtered. Slow evaporation of the filtrate produced prismatic dark red crystals within 4 days. Yield: 66%. Elemental analysis for the compound dried overnight under reduced pressure: calcd. For **1**-4MeOH (formula $Fe_4O_{17}Cl_2C_{60}H_{52}N_{12}$) C 47.81, H 3.48, N 11.15; found: C 47.36, H 3.57, N 10.88. IR analysis (neat, cm^{-1}): 2691 (b), 1602 (m), 1582 (m), 1526 (m), 1468 (m), 1428 (s), 1394 (m), 1329 (m), 1198 (m), 1146 (m), 1033 (s), 744 (s).

The use of $Fe^{III}(ClO_4)_3$ as iron(III) source does not result in the isolation of the Fe_4 cluster; it appears that the gradual in situ generation of iron(III) ions from the aerobic oxidation of Fe^{II} is important for the formation of the cluster.

(24) Wang, Q. X.; Jiao, K.; Sun, W.; Jian, F. F.; Hu, X. *Eur. J. Inorg. Chem.* **2006**, 1838–1845.
(25) Roy, M.; Bhowmick, T.; Santhanagopal, R.; Ramakumar, S.; Chakravarty, A. R. *Dalton Trans.* **2009**, 4671–4682.
(26) Saalfrank, R. W.; Trummer, S.; Krautscheid, H.; Schunemann, V.; Trautwein, A. X.; Hien, S.; Stadler, C.; Daub, J. *Angew. Chem., Int. Ed. Engl.* **1996**, *35*, 2206–2208.
(27) Overgaard, J.; Larsen, F. K.; Schiott, B.; Iversen, B. B. *J. Am. Chem. Soc.* **2003**, *125*, 11088–11099.
(28) Gass, I. A.; Milios, C. J.; Collins, A.; White, F. J.; Budd, L.; Parsons, S.; Murrie, M.; Perlepes, S. P.; Brechin, E. K. *Dalton Trans.* **2008**, 2043–2053.
(29) Veith, M.; Gratz, F.; Huch, V. *Eur. J. Inorg. Chem.* **2001**, 367–368.
(30) Kusserow, M.; Spandl, J. *Z. Anorg. Allg. Chem.* **2006**, *632*, 885–892.
(31) O'Keefe, B. J.; Monnier, S. M.; Hillmyer, M. A.; Tolman, W. B. *J. Am. Chem. Soc.* **2001**, *123*, 339–340.
(32) Spandl, J.; Kusserow, M.; Brudgam, I. *Z. Anorg. Allg. Chem.* **2003**, *629*, 968–974.
(33) Caneschi, A.; Cornia, A.; Lippard, S. J.; Papaefthymiou, G. C.; Sessoli, R. *Inorg. Chim. Acta* **1996**, *243*, 295–304.
(34) Cotton, F. A.; Daniels, L. M.; Jordan, G. T.; Murillo, C. A.; Pascual, I. *Inorg. Chim. Acta* **2000**, *297*, 6–10.
(35) Cotton, F. A.; Daniels, L. M.; Falvello, L. R.; Matonic, J. H.; Murillo, C. A.; Wang, X.; Zhou, H. *Inorg. Chim. Acta* **1997**, *266*, 91–102.
(36) Jian, F. F.; Xiao, H. L.; Bai, Z. S.; Zhao, P. *J. Mater. Chem.* **2006**, *16*, 3746–3752.
(37) Canada-Vilalta, C.; O'Brien, T. A.; Pink, M.; Davidson, E. R.; Christou, G. *Inorg. Chem.* **2003**, *42*, 7819–7829.
(38) Reis, D. M.; Nunes, G. G.; Sa, E. L.; Friedermann, G. R.; Mangrich, A. S.; Evans, D. J.; Hitchcock, P. B.; Leigh, G. J.; Soares, J. F. *New J. Chem.* **2004**, *28*, 1168–1176.
(39) Kahn, O. *Molecular Magnetism*; Wiley-VCH: New York, 1993.

Table 1. Crystal Data and Structure Refinement for $[Fe_4O(OCH_3)_4(\mathbf{bisi})_4](ClO_4)_2\cdot 4CH_3OH$ (**1**)

empirical formula	$C_{64}H_{68}Cl_2Fe_4N_{12}O_{21}$
F_w (g mol^{-1})	1635.60
crystal system	tetragonal
space group	$I4_1/a$
crystal color	red
temperature (K)	173(2)
a (Å)	13.401(2)
b (Å)	13.401(2)
c (Å)	37.099(3)
$\alpha = \beta = \gamma$ (deg)	90
V (Å^3)	6662.7(1)
ρ_{calcd} (Mg/m^3)	1.631
μ (mm^{-1})	1.021
$F(000)$	3368
θ for data collection (deg)	4.16−20.87
collected reflections	57015
independent reflections	3809
R_{int}	0.0525
$R\,[I > 2\sigma(I)]$	0.0517
wR (all data)	0.1505
goodness of fit on F^2	1.100
largest diff. peak and hole (e Å^3)	0.945 and −0.857

X-ray Crystallographic Analysis and Data Collection. Crystallographic data and refinement details are given in Table 1. A single crystal was selected for the X-ray measurements and mounted to the glass fiber using the oil drop method,[40] and data were collected at 173(2) K on a Nonius Kappa CCD diffractometer (Mo Kα radiation, graphite monochromator, $\lambda = 0.71073$). The intensity data were corrected for Lorentz and polarization effects and for absorption. The programs COLLECT,[41] SHELXS-97,[42] and SHELXL-97[43] were used for data reduction, structure solution, and structure refinement, respectively. The disordered perchlorate anion was refined as a rigid group in the two positions with population parameter 0.5. The non-hydrogen atoms were refined anisotropically. The H atoms were geometrically fixed and allowed to ride on the attached atoms.

Results and Discussion

Crystal Structure of $[Fe_4(\mu_4\text{-}O)(\mu\text{-}MeO)_4(\mathbf{bisi})_4](ClO_4)_2\cdot 4MeOH$ (1). Reaction of 1 equiv of iron(II) perchlorate hexahydrate with 1 equiv of ligand **Hbisi** in methanol under aerobic conditions produces dark red crystals of **1** after 4 days, with a yield of 66%. Single-crystal X-ray studies revealed that **1** crystallizes in the tetragonal space group $I4_1/a$. A view of the cationic part of **1** is represented in Figure 1. Details for the structure solution and refinement are summarized in Table 1, and selected bond distances and angles are given in Table 2. The core of the tetranuclear compound **1** is composed of four symmetry-related six-coordinated iron(III) ions (resulting from the aerobic oxidation of the initial iron(II) ions) identified as Fe1, Fe1a, Fe1b, and Fe1c (Figure 1A; symmetry operations: a, 1/4+x, 5/4−y, 1/4−z; b, 1−x, 3/2−y, z; c, 5/4−x, 1/4+y, 1/4−z). Fe1 is in a distorted octahedral coordination environment (Figure 1B), with four oxygen atoms in a plane and two axial nitrogen atoms. The latter come from the imine nitrogen (N17c) and the benzimidazolyl nitrogen (N8) belonging to two

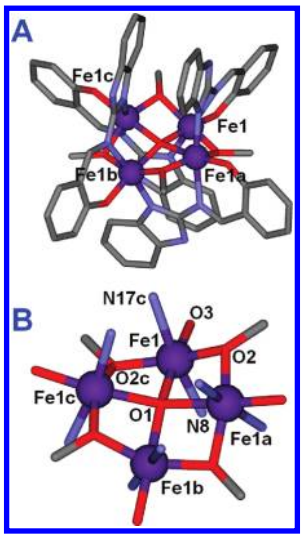

Figure 1. (A) Illustration of the tetrairon(III) cation in $[Fe_4O(OCH_3)_4(\mathbf{bisi})_4](ClO_4)_2\cdot 4CH_3OH$ (**1**). Hydrogen atoms, perchlorate anions, and lattice methanol molecules are omitted for clarity. Symmetry operations: a, 1/4+x, 5/4−y, 1/4−z; b, 1−x, 3/2−y, z; c, 5/4−x, 1/4+y, 1/4−z. (B). Tetranuclear core of **1** with the atom numbering scheme for one of the four crystallographically equivalent iron centers.

Table 2. Selected Bond Distances (Angstroms) and Angles (Degrees) for $[Fe_4O(OCH_3)_4(\mathbf{bisi})_4](ClO_4)_2\cdot 4CH_3OH$ (**1**)[a]

Fe1			
Fe1−O1	2.082(2)	O1−Fe1−O2	81.08(7)
Fe1−O2	1.947(2)	O2−Fe1−O3	99.75(11)
Fe1−O3	1.913(3)	O3−Fe1−O2c	101.11(11)
Fe1−N8	2.232(3)	O2c−Fe1−O1	80.48(7)
Fe1−O2c	1.972(2)	N8−Fe1−N17c	171.09(10)
Fe1−N17c	2.134(3)	Fe1−O2c−Fe1c	99.53(11)
Fe1···Fe1c	2.992(1)	Fe1−O1−Fe1b	159.07(2)

[a] Symmetry operations: b, 1−x, 3/2−y, z; c, 5/4−x, 1/4+y, 1/4−z.

different **bisi** ligands connecting Fe1 to Fe1a and Fe1c, respectively. Within the O_4 plane, one diagonal square includes two μ-MeO^- ligands (oxygen atoms O2 and O2c) bridging Fe1 to Fe1a and Fe1c, respectively, while the second one contains one **bisi** phenoxido ligand (oxygen atom O3), and the μ_4-oxido ligand (oxygen atom O1), linking all four iron centers (Figure 1). The Fe−N bond lengths (Table 2) can be considered as normal for this type of FeN_2O_4 coordination unit.[44] The $Fe-O_{MeO}$ and $Fe-O_{oxido}$ bond distances are in normal ranges,[45,46] as is the $Fe-O_{PhO}$ bond length.[28] The basal coordination angles, ranging from 80.48(7) to 101.11(11)°, reflect the distortion of the octahedron which is most likely due to steric constraints induced both by the dinucleating coordination of the **bisi** ligands and by the μ-methoxido ligands. This octahedral distortion is indicated as well by the strong deformation of the fully π-conjugated **bisi** ligand, upon coordination to two iron(III) ions. Actually,

(40) Kottke, T.; Stalke, D. *J. Appl. Crystallogr.* **1993**, *26*, 615–619.
(41) *COLLECT*; Nonius B. V.: Delft, The Netherlands, 2002.
(42) Sheldrick, G. M. *SHELXS-97 Program for Crystal Structure Determination*; University of Göttingen: Göttingen, Germany, 1997.
(43) Sheldrick, G. M. *SHELXL-97-2, Program for Crystal Structure Refinement*; University of Göttingen: Göttingen, Germany, 1997.
(44) Gass, I. A.; Milios, C. J.; Whittaker, A. G.; Fabiani, F. P. A.; Parsons, S.; Murrie, M.; Perlepes, S. P.; Brechin, E. K. *Inorg. Chem.* **2006**, *45*, 5281–5283.
(45) Shaw, R.; Laye, R. H.; Jones, L. F.; Low, D. M.; Talbot-Eeckelaers, C.; Wei, Q.; Milios, C. J.; Teat, S.; Helliwell, M.; Raftery, J.; Evangelisti, M.; Affronte, M.; Collison, D.; Brechin, E. K.; McInnes, E. J. L. *Inorg. Chem.* **2007**, *46*, 4968–4978.
(46) Hegetschweiler, K.; Schmalle, H. W.; Streit, H. M.; Gramlich, V.; Hund, H. U.; Erni, I. *Inorg. Chem.* **1992**, *31*, 1299–1302.

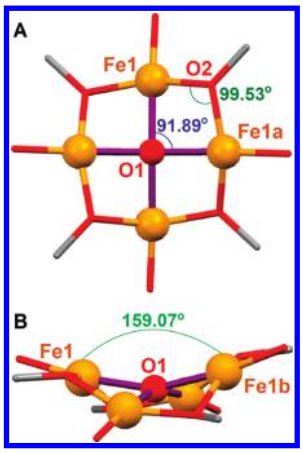

Figure 2. Illustrations of the $Fe_4(\mu_4\text{-O})$ core showing (A) its square geometry with Fe−O2−Fe angles of 99.53(11)° and $Fe_1-O_1-Fe_{1a}$ angles of 91.89(2)°; (B) the tetrahedral distortion of the square plane characterized by Fe−O1−Fe angles of 159.07(2)°. Symmetry operations: a, $1/4+x$, $5/4-y$, $1/4-z$; b, $1-x$, $3/2-y$, z.

the plane containing the benzimidazole unit and the plane including the salicylaldimine group of **bisi** make an angle of 22°, significantly away from planarity (see Supporting Information, Figure S1). As a consequence, the $Fe_4(\mu_4\text{-O})$ unit is not perfectly square planar and exhibits a tetrahedral distortion with a dihedral angle within the Fe_4 unit of 28.36(2)° and Fe−O1−Fe angles of 159.07(2)° (Figure 2 and Table 2), 20.93° outside the ideal value of 180°. Therefore, each iron(III) atom exhibits two kinds of connections with neighboring atoms. A first connection type occurs between each iron center and two vicinal neighbors (Fe1 and Fe1a, Figure 2A) through the μ_4-oxido O1 and the μ_2-methoxido O2 donors, with acute angles (Fe1−O1−Fe1a = 91.89(2)° and Fe1−O2−Fe1a = 99.53(11)°). The second connection links two opposite iron atoms (Fe1 and Fe1b, Figure 2B) through the μ_4-oxido O1 bridge (Fe1−O1−Fe1b = 159.07(2)°).

$Fe_4(\mu_4\text{-O})$ Motifs Found in the Literature. The occurrence of the μ_4-oxido tetrairon unit featured in **1** has been searched in the Cambridge Structural Database (CSD version 5.30; November 2008 + 3 updates). A total of 71 single-crystal X-ray structures containing the $Fe_4(\mu_4\text{-O})$ motif have been found (see Table S1 in the Supporting Information for all the corresponding CSD refcodes). From these 71 compounds, only 3 exhibit *discrete* $Fe^{II}_4(\mu_4\text{-O})$ units (HEQVAB,[36] NEKXOQ,[35] and XIRFIN[34]). A fourth compound, namely, $[H_3NCH_2CH_2NH_3]_2[Fe_4O(PO_4)_4]\cdot H_2O$ (CSD refcode SINVAM),[47] contains mixed-valent $Fe^{II,III}_4(\mu_4\text{-O})$ motifs which are linked by phosphate groups, generating a three-dimensional open coordination polymer (Supporting Information, Figure S2). Representations of the core of the three compounds HEQVAB, NEKXOQ, and SINVAM are shown in Figure 3, which illustrate the occurrence of tetrahedral $Fe_4(\mu_4\text{-O})$ entities. Unfortunately, for XIRFIN, the atomic coordinates are not available, and therefore the representation of its $Fe_4(\mu_4\text{-O})$ core cannot be sketched. However, Cotton et al.[34] have shown that this tetrairon(II) unit is tetrahedral as well. Thus, the present $Fe^{III}_4(\mu_4\text{-O})$ unit (Figure 2) corresponds to the first *isolated* μ_4-oxido iron(III) system reported so far, which moreover exhibits an almost square-planar geometry.

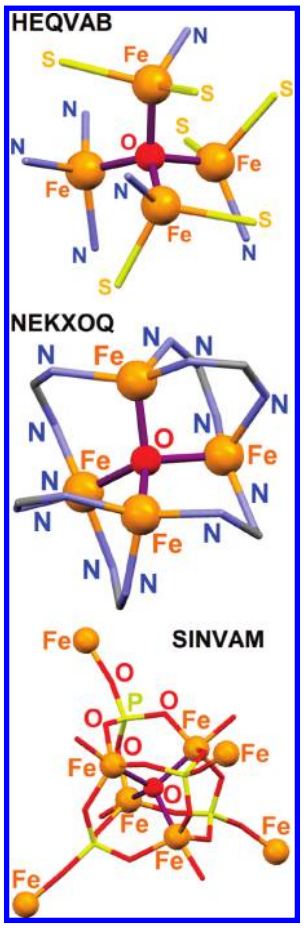

Figure 3. Representations of the $Fe_4(\mu_4\text{-O})$ core for HEQVAB,[36] NEKXOQ,[35] and SINVAM.[47] The $Fe_4(\mu_4\text{-O})$ unit is symbolized by purple Fe−O bonds. For SINVAM, only one phosphate group has been labeled for clarity.

Table 3. Fe_n Cluster Compounds Exhibiting the $Fe_4(\mu_4\text{-O})$ Motif with the Corresponding References[a]

Fe_n cluster	number of structures	references
Fe_5	11	30,31,38,57
Fe_6	13	7,28,32,37,46,58−65
Fe_7	1	66
Fe_8	22	22,28,44,67−77
Fe_9	3	29,30,78
Fe_{10}	5	3,66,79−81
Fe_{12}	3	9,33,82
Fe_{13}	1	83
Fe_{14}	3	45,84
Fe_{17}	4	85−87
Fe_{22}	1	88

[a] See also Figures S3−S10 in the Supporting Information.

The remaining 67 structures include the $Fe_4(\mu_4\text{-O})$ motif as part of higher-nuclearity clusters (Supporting Information, Table S1). Hence, the $Fe_4(\mu_4\text{-O})$ group is observed in Fe_5, Fe_6, Fe_7, Fe_8, Fe_9, Fe_{10}, Fe_{12}, Fe_{13}, Fe_{14}, Fe_{17}, and Fe_{22} cluster compounds (see Table 3). A representative example for each Fe_n series is depicted in Figure 4 (all other structures are illustrated in Supporting Information, Figures S3−S10).

Magnetic Properties. The magnetic susceptibility of compound **1** was measured in the range 2−300 K under

(47) DeBord, J. R. D.; Reiff, W. M.; Warren, C. J.; Haushalter, R. C.; Zubieta, J. *Chem. Mater.* **1997**, *9*, 1994–1998.

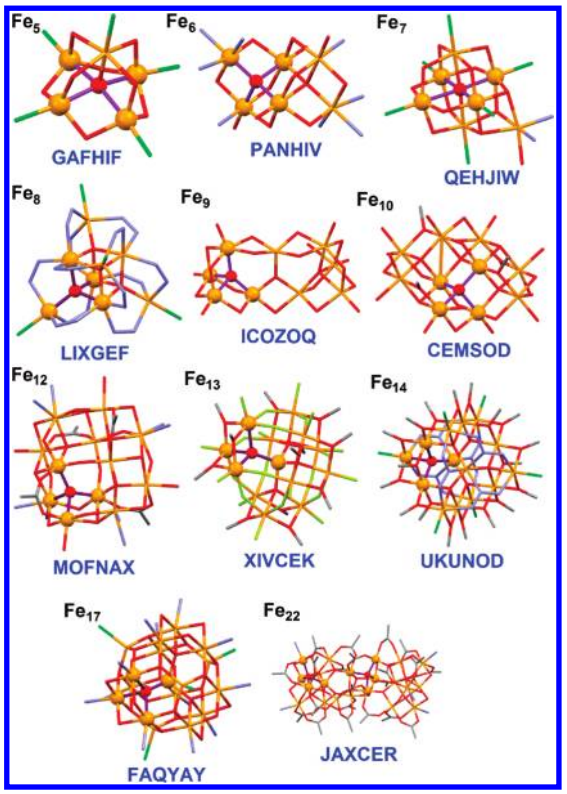

Figure 4. Illustrative examples of Fe_n cores exhibiting the $Fe_4(\mu_4\text{-O})$ motif with the corresponding CSD refcode. The $Fe_4(\mu_4\text{-O})$ unit is highlighted by atoms drawn in the ball and stick mode and by purple Fe−O bonds.

a constant magnetic field of 0.5 T (see Figure 5 and Supporting Information, Figure S11). These data have been corrected from a mononuclear high-spin Fe(III) impurity representing less than 1% of the total number of iron ions in the investigated sample (see Supporting Information). At room temperature, the $\chi_M T$ product is 8.87 $cm^3 \cdot K \cdot mol^{-1}$, well below the 17.5 $cm^3 \cdot K \cdot mol^{-1}$ value that is expected for a tetranuclear species containing four non-interacting high-spin Fe(III) centers ($S_i = 5/2$ and $g = 2$). When the temperature is lowered, the $\chi_M T$ product decreases continuously to reach a plateau at zero below 10 K. These data characterize an antiferromagnetic exchange interaction between the metal centers, leading to an $S = 0$ ground state.

Inspection of the molecular structure of **1** highlights the presence of two types of coupling constants, namely, J_1 and J_2. The former describes the exchange coupling through the doubly bridged μ_4-oxido-μ-methoxido bridging pattern along the edges of the Fe_4 square, whereas J_2 corresponds to the diagonal exchange pathway via the singly bridged μ_4-O^{2-} unit (Inset in Figure 5). The Heisenberg Hamiltonian resulting from that scheme is given in eq 1.

$$H = -2J_1(S_1 \cdot S_2 + S_2 \cdot S_3 + S_3 \cdot S_4 + S_4 \cdot S_1) - 2J_2(S_1 \cdot S_3 + S_2 \cdot S_4) \quad (1)$$

where the iron centers have been labeled with the subscripts 1, 2, 3, and 4 in place of 1, 1a, 1b, and 1c used for the structure description, respectively. The energy levels resulting from this exchange-coupling scheme can be

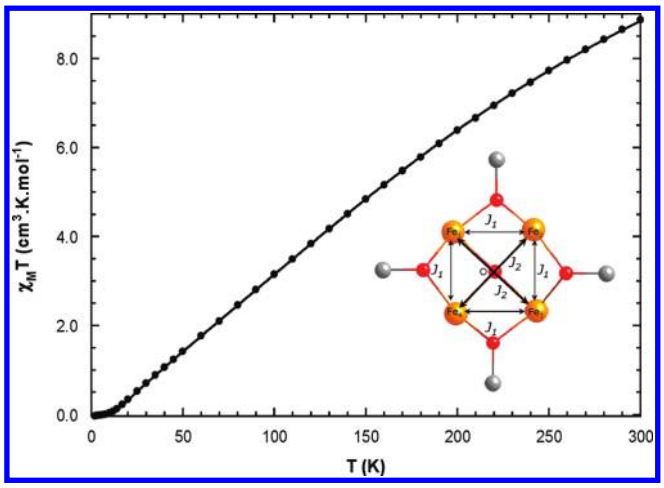

Figure 5. Variations of the molar magnetic susceptibility of **1** upon temperature drawn as the $\chi_M T$ vs T curve (full circles). The theoretical curve was obtained using $g = 2.00$, $J_1 = -1.4\ cm^{-1}$, and $J_2 = -19.2\ cm^{-1}$ (solid line). The inset shows the coupling scheme within the $[Fe_4(\mu_4\text{-O})(\mu\text{-OMe})_4]^{6+}$ core.

labeled with the total spin S and the two subspins S_{13} and S_{24} of the pairs along the diagonals (eq 2).

$$E(S_{13}, S_{24}, S) = -J_1 S(S+1) - (J_2 - J_1)[S_{13}(S_{13}+1) + S_{24}(S_{24}+1)] \quad (2)$$

The data illustrated in Figure 5 could be satisfyingly reproduced using the van Vleck formula associated with the spin energies given in eq 2, assuming a spin independent g-factor (see Supporting Information). The zero-field splitting of the high-spin Fe(III) sites has been neglected. The best fit leads to $J_1 = -1.4(4)\ cm^{-1}$ and $J_2 = -19.2(3)\ cm^{-1}$, assuming $g = 2.00$.

These J values clearly establish that the magnetic-exchange interaction is stronger between opposite iron ions (Fe1−Fe1b and Fe1a−Fe1c) than between vicinal ones (Fe1−Fe1a, Fe1a−Fe1b, Fe1b−Fe1c and Fe1c−Fe1). This feature is consistent with rationalizations provided by magneto-structural correlations reported in the literature that have established that J depends both on the bridging angle Fe−O−Fe and on the mean Fe−O distance within the bridging unit.[48] Indeed, in the case of the μ-oxidodiiron(III) system, both a short Fe−O bond and a large Fe−O−Fe angle favor a strong interaction and a large $|J|$ that can reach a few hundred wavenumbers.[49,50] Therefore, the present moderate value of $|J_2|$ is due to the combination of a large bridging angle (159°) and a long Fe−O distance (2.08 Å). The bridging pattern of the vicinal iron ions involves both the μ_4-oxido and the μ_2-methoxido ligands. The contribution of the μ_4-oxido bridge to $|J_1|$ is certainly lessened when compared to $|J_2|$, because the bridging angle is now drastically reduced to about 92° (from 159°). On the other hand, the methoxido bridges are less efficient than the oxido ones to mediate antiferromagnetic interactions. This was shown by Gatteschi et al. who developed a correlation between $|J|$ and the bridging angle for

(48) Weihe, H.; Güdel, H. U. *J. Am. Chem. Soc.* **1997**, *119*, 6539–6543.
(49) Murray, K. S. *Coord. Chem. Rev.* **1974**, *12*, 1–35.
(50) Kurtz, D. M. *Chem. Rev.* **1990**, *90*, 585–606.

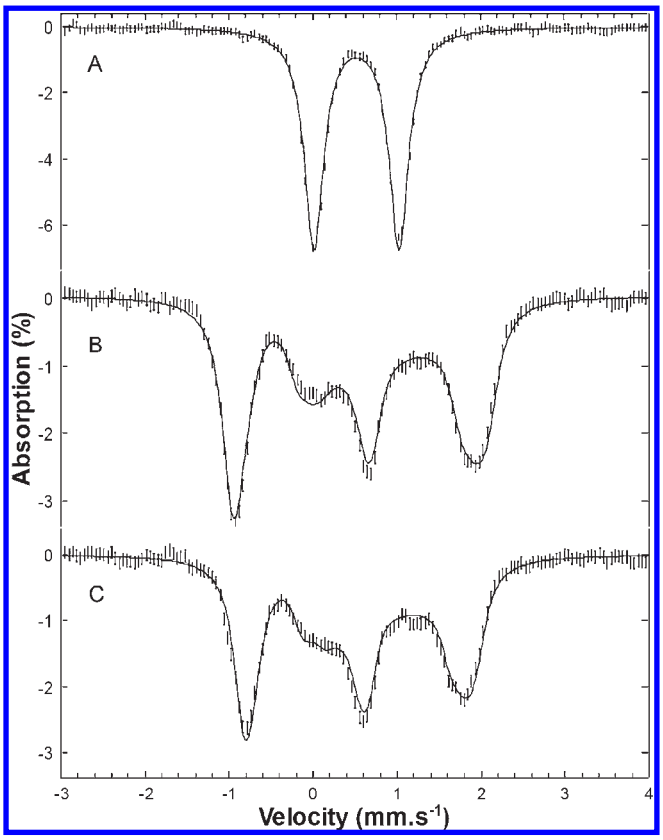

Figure 6. Experimental Mössbauer spectra recorded at (A) zero field and 4.2 K or in a 7 T external field applied parallel to the γ-beam at (B) 4.2 K or (C) 50 K (hatched marks). Simulations (solid lines) were obtained in the fast relaxation mode assuming a unique $S = 0$ system (traces A and B) or a symmetric dinuclear system with 5/2 local spins (traces A, B and C) with the following parameters $\delta = 0.515$ mm.s^{-1}, $\Delta E_Q = 1.011$ mm.s^{-1}, $\eta = 0.33$, $\Gamma_{fwhm} = 0.28$ mm.s^{-1}, $J_2 = -18.4$ cm^{-1} and $a_{iso} = -20.12$ T.

diiron(III) complexes bridged by two methoxides.[51] For the present bridging angle (Fe1−O2−Fe1a = 99.53(11)°), an antiferromagnetic contribution of 3 cm^{-1} can be estimated per methoxido bridge that is consistent with the experimental value of $J_1 = -1.4$ cm^{-1}.

Mössbauer Studies. The spectra recorded at 4.2 K are shown in Figure 6 (traces A and B). In zero-field (Figure 6, trace A), a unique quadrupole doublet was observed, indicating that the four iron nuclei of compound **1** are equivalent. It may be added that the paramagnetic impurity revealed by the magnetic susceptibility is not detectable; this is not surprising owing to the fact that it represents less than 1% in iron atom constitution. The spectra recorded at zero field (Figure 6, trace A) and under a 7 T magnetic field parallel to the γ-beam (Figure 6, trace B) can be interpreted assuming a diamagnetic behavior for compound **1**, in agreement with the magnetic susceptibility data. The simulations shown in Figure 6 (traces A and B, solid lines) were obtained with the following parameters: $\delta = 0.515(10)$ mm·s^{-1}, $\Delta E_Q = 1.011(15)$ mm·s^{-1}, $\eta = 0.33(5)$ and $\Gamma_{fwhm} = 0.28(2)$ mm·s^{-1}. The value of the isomer shift is perfectly in agreement with the expected value for a high spin Fe(III) ion,[52] and is in the range 0.35−0.60 mm·s^{-1}, which is typical for 5- or 6-coordinate high-spin diiron(III) μ-oxido species. On the other hand, the quadrupole splitting value is intermediate between the values observed for oxido and carboxylato bridged diiron(III) species,[49,50] and those obtained for ferritin and high-nuclearity clusters.[9] It can be argued that the lengthening of the Fe-(μ_4-O) distance in **1** and high-nuclearity clusters or ferritin will lower the covalency of the oxido ligand that in turn will diminish the quadrupole splitting of the iron ions.

To get further insights in the properties of compound **1**, spectra were also recorded at 25, 35, and 50 K. The zero-field spectra recorded at 4.2 and 25 K are superimposable (see Supporting Information, Figure S12), thus indicating no significant changes in the isomeric shift and the quadrupole splitting of the iron nuclei upon raising the temperature. The spectra recorded in the presence of an external 7 T magnetic field parallel to the γ-rays (Figure 6, trace C and Supporting Information, Figure S13) show a narrowing of the Mössbauer signature that is slightly increased with the temperature. This narrowing may be attributed to the increased population of the paramagnetic excited states of compound **1** (see below).

Modelization of the Electronic Structure of Coordination Compound 1. The analysis of the variations of the magnetic susceptibility with the temperature suggests a moderate antiferromagnetic interaction through the μ_4-oxido bridge and a weak antiferromagnetic exchange inside the [Fe(μ_4-O)(μ-OMe)Fe] units. Since the strongest couplings involves Fe_1 and Fe_3 on one hand and Fe_2 and Fe_4 on the other, the electronic structure of compound **1** can be well interpreted by referring to the spin ladder of two identical, antiferromagnetically coupled diiron(III) units (namely, Fe_1−Fe_3 and Fe_2−Fe_4; Scheme 2). In addition, as mentioned above, the spins of these pairs are good quantum numbers because of the symmetry of the coordination compound.

For two local 5/2 electronic spins, the total spin S of the pair can vary between 0 and 5 with the energy levels ordering according to the well-known $-JS(S+1)$ law (left part of Scheme 2). When two such pairs coexist without extra interaction, the spin levels are organized according to the spin value within each pair (central part of Scheme 2). For a (S_{13}, S_{24}) set, the levels associated with the total spin S ranging from $|S_{13}-S_{24}|$ to $S_{13}+S_{24}$ are degenerated. This degeneracy is removed by the exchange interaction occurring along the edges of the tetranuclear Fe square (right part of Scheme 2). It can be noticed that there is no effect of J_1 on the ground state ($S = 0$, not degenerated) and on the first excited state ($S = 1$, doubly degenerated), where one diiron(III) pair at least is diamagnetic. Starting from the ground state and looking to higher energy levels, the first effect of J_1 will concern the ($S_{13} = 1, S_{24} = 1$) spin levels lying in average at 76.8 cm^{-1} from the ground state. In addition, the splitting ($6J_1$) does not exceed 10 cm^{-1}.

Owing to the fact that J_1 operates only on excited states above 70 cm^{-1} and that its effect on the lowest one is small ($\leq$10 cm^{-1}), it is reasonable to neglect it ($J_1 = 0$ cm^{-1}) to analyze the Mössbauer spectra recorded between 4 and 50 K. Compound **1** will thus be modeled by a single symmetric diiron(III) unit (Fe_1−Fe_3 or Fe_2−Fe_4).

(51) LeGall, F.; deBiani, F. F.; Caneschi, A.; Cinelli, P.; Cornia, A.; Fabretti, A. C.; Gatteschi, D. *Inorg. Chim. Acta* **1997**, *262*, 123–132.
(52) Greenwood, N. N.; Gibb, T. C. *Mössbauer Spectroscopy*; Chapman and Hall, Ltd.: London, 1971.

Scheme 2. Spin Level Energies As a Function of the Exchange Coupling Constants [a]

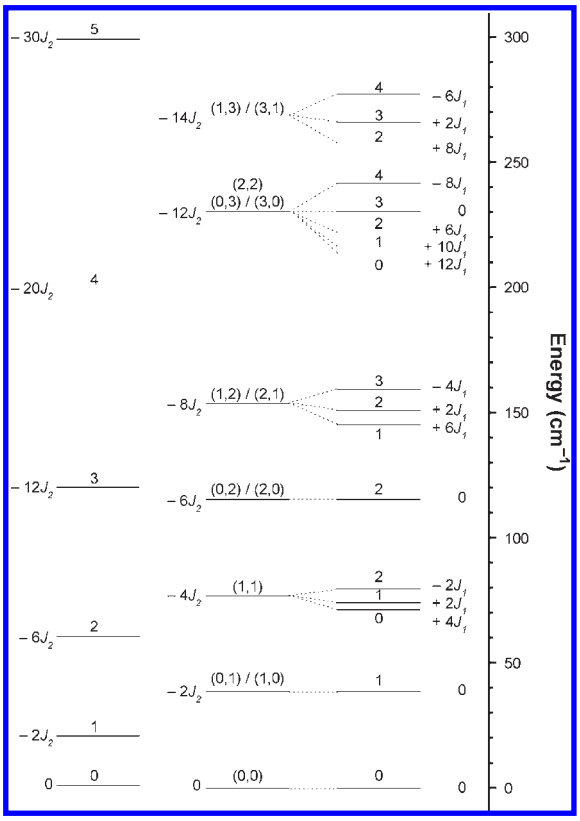

[a] Left: for a dinuclear system with two 5/2 local spins coupled through J_2. The energy and the total spin value are indicated on the left and above the level, respectively. Central part: for two identical dinuclear units with two 5/2 local spins coupled through J_2. The energy and the spin of the pairs are indicated on the left and above the spin level as (S_{13}, S_{24}), respectively (the full spin ladder is given in the Supporting Information). Right part: influence of the J_1-coupling occurring on the square edges in **1**. The total spin value is indicated above the level and the incremented energy on the right. The energy scale in wavenumbers applies to the central and right parts of the scheme taking $J_1 = -1.4$ cm^{-1} and $J_2 = -19.4$ cm^{-1}.

Because of the identical zero-field Mössbauer signatures at 4.2 and 25 K, the isomeric shift δ, the quadrupole splitting ΔE_Q, and the rhombicity parameter η of the iron centers along with the line width Γ_{fwhm} were fixed to their values determined at 4.2 K (see above). The narrowing of the signature observed upon increasing the temperature suggests a fast relaxation mode with a negative hyperfine coupling constant. In contrast with the diamagnetic ground state, the paramagnetic excited states are characterized by a non-zero electronic spin density on the iron centers (namely, 1/2 whatever the total spin value), that leads on the iron nucleus to an induced magnetic field that is opposite to the external 7 T applied field. Therefore, the total magnetic field experienced by an iron nucleus is 7 T in the diamagnetic ground state but lower in the paramagnetic excited states. This lowering leads to a narrowing of the Mössbauer spectrum that is all the more marked that the population of the excited states increases with increasing temperatures. Assuming an isotropic hyperfine interaction (a_{iso}), a simultaneous fit of the spectra recorded at 4.2, 25, 35, and 50 K with a 7 T magnetic field thus led to $J = -18.4(15)$ cm^{-1} and $a_{iso} = -20(3)$ T. The corresponding theoretical spectrum is shown at 50 K (see Figure 6, trace C). The obtained J-value is well in agreement with the one obtained from the SQUID measurements. Moreover, the hyperfine coupling constant value falls well in the range obtained for hexacoordinated high-spin Fe(III) ions.[53−56] It may be noticed that the a_{iso}-value is correlated to the J-value.

(53) Schünemann, V.; Paulsen, H. *Mössbauer Spectroscopy, in Applications of Physical Methods to Inorganic and Bioinorganic Chemistry*; Wiley: New York, 2007; pp 243−270.
(54) Fox, B. G.; Hendrich, M. P.; Surerus, K. K.; Andersson, K. K.; Froland, W. A.; Lipscomb, J. D.; Munck, E. *J. Am. Chem. Soc.* **1993**, *115*, 3688–3701.
(55) Hendrich, M. P.; Day, E. P.; Wang, C. P.; Synder, B. S.; Holm, R. H.; Munck, E. *Inorg. Chem.* **1994**, *33*, 2848–2856.
(56) Kauffmann, K. E.; Popescu, C. V.; Dong, Y. H.; Lipscomb, J. D.; Que, L.; Munck, E. *J. Am. Chem. Soc.* **1998**, *120*, 8739–8746.
(57) Veith, M.; Gratz, F.; Huch, V.; Gutlich, P.; Ensling, A. *Z. Anorg. Allg. Chem.* **2004**, *630*, 2329–2336.
(58) Jiang, G.; Bai, J.; Xing, H.; Li, Y.; You, X. *Cryst. Growth Des.* **2006**, *6*, 1264–1266.
(59) Hegetschweiler, K.; Schmalle, H.; Streit, H. M.; Schneider, W. *Inorg. Chem.* **1990**, *29*, 3625–3627.
(60) Burkill, H. A.; Robertson, N. R.; Vilar, R.; White, A. J. P.; Williams, D. J. *Inorg. Chem.* **2005**, *44*, 3337–3346.
(61) Seddon, E. J.; Huffman, J. C.; Christou, G. *J. Chem. Soc., Dalton Trans.* **2000**, 4446–4452.
(62) Kiskin, M. A.; Aleksandrov, G. G.; Shvedenkov, Y. G.; Novotortsev, V. M.; Eremenko, I. L. *Russ. Chem. Bull.* **2006**, 900.
(63) Cornia, A.; Gatteschi, D.; Hegetschweiler, K.; HausherrPrimo, L.; Gramlich, V. *Inorg. Chem.* **1996**, *35*, 4414–4419.
(64) Chae, H. K.; Hwang, C.; Dong, Y.; Yun, H.; Jang, H. G. *Chem. Lett.* **2000**, 992–993.
(65) Dolbecq, A.; Compain, J. D.; Mialane, P.; Marrot, J.; Riviere, E.; Secheresse, F. *Inorg. Chem.* **2008**, *47*, 3371–3378.
(66) Finn, R. C.; Zubieta, J. *J. Clust. Sci.* **2000**, *11*, 461–482.
(67) Baran, P.; Boca, R.; Chakraborty, I.; Giapintzakis, J.; Herchel, R.; Huang, Q.; McGrady, J. E.; Raptis, R. G.; Sanakis, Y.; Simopoulos, A. *Inorg. Chem.* **2008**, *47*, 645–655.
(68) Ammala, P.; Cashion, J. D.; Kepert, C. M.; Moubaraki, B.; Murray, K. S.; Spiccia, L.; West, B. O. *Angew. Chem., Int. Ed.* **2000**, *39*, 1688–1690.
(69) Raptis, R. G.; Georgakaki, I. P.; Hockless, D. C. R. *Angew. Chem., Int. Ed.* **1999**, *38*, 1632–1634.
(70) Jones, L. F.; Jensen, P.; Moubaraki, B.; Berry, K. J.; Boas, J. F.; Pilbrow, J. R.; Murray, K. S. *J. Mater. Chem.* **2006**, *16*, 2690–2697.
(71) Dellamico, D. B.; Calderazzo, F.; Labella, L.; Maichlemossmer, C.; Strahle, J. *J. Chem. Soc., Chem. Commun.* **1994**, 1555–1556.
(72) Prakash, R.; Saalfrank, R. W.; Maid, H.; Scheurer, A.; Heinemann, F. W.; Trautwein, A. X.; Bottger, L. H. *Angew. Chem., Int. Ed.* **2006**, *45*, 5885–5889.
(73) Nair, V. S.; Hagen, K. S. *Inorg. Chem.* **1994**, *33*, 185–186.
(74) Hahn, F. E.; Jocher, C.; Lugger, T. *Z. Naturforsch., B: Chem. Sci.* **2004**, *59*, 855–858.
(75) Ako, A. M.; Waldmann, O.; Mereacre, V.; Klower, F.; Hewitt, I. J.; Anson, C. E.; Gudel, H. U.; Powell, A. K. *Inorg. Chem.* **2007**, *46*, 756–766.
(76) Liu, T.; Zhang, Y. J.; Wang, Z. M.; Gao, S. *J. Am. Chem. Soc.* **2008**, *130*, 10500–10501.
(77) Stamatatos, T. C.; Christou, A. G.; Mukherjee, S.; Poole, K. M.; Lampropoulos, C.; Abboud, K. A.; O'Brien, T. A.; Christou, G. *Inorg. Chem.* **2008**, *47*, 9021–9034.
(78) Godin, B.; Chen, Y. G.; Vaissermann, J.; Ruhlmann, L.; Verdaguer, M.; Gouzerh, P. *Angew. Chem., Int. Ed.* **2005**, *44*, 3072–3075.
(79) Godbole, M. D.; Roubeau, O.; Mills, A. M.; Kooijman, H.; Spek, A. L.; Bouwman, E. *Inorg. Chem.* **2006**, *45*, 6713–6722.
(80) Dell'Amico, D. B.; Boschi, D.; Calderazzo, F.; Ianelli, S.; Labella, L.; Marchetti, F.; Pelizzi, G.; Quadrelli, E. G. F. *Inorg. Chim. Acta* **2000**, *300*, 882–891.
(81) Asirvatham, S.; Khan, M. A.; Nicholas, K. M. *Inorg. Chem.* **2000**, *39*, 2006–2007.
(82) Bagai, R.; Daniels, M. R.; Abboud, K. A.; Christou, G. *Inorg. Chem.* **2008**, *47*, 3318–3327.
(83) Bino, A.; Ardon, M.; Lee, D.; Spingler, B.; Lippard, S. J. *J. Am. Chem. Soc.* **2002**, *124*, 4578–4579.
(84) Low, D. M.; Jones, L. F.; Bell, A.; Brechin, E. K.; Mallah, T.; Riviere, E.; Teat, S. J.; McInnes, E. J. L. *Angew. Chem., Int. Ed.* **2003**, *42*, 3781–3784.
(85) Evangelisti, M.; Candini, A.; Ghirri, A.; Affronte, M.; Powell, G. W.; Gass, I. A.; Wood, P. A.; Parsons, S.; Brechin, E. K.; Collison, D.; Heath, S. L. *Phys. Rev. Lett.* **2006**, *97*, 167202.

Indeed, when the exchange interaction increases, the observed hyperfine constant becomes more negative to compensate for the decrease in the population of at least the first paramagnetic excited spin state.

The results described above clearly show that the temperature dependence of the magnetic susceptibility and of the Mössbauer signatures are in total agreement, and that in a first approximation, the system can be considered as two identical Fe(III) pairs, while neglecting the vicinal magnetic interaction.

Concluding Remarks

The isolation of $[Fe_4(\mu_4\text{-}O)(\mu\text{-}MeO)_4(bisi)_4](ClO_4)_2 \cdot 4MeOH$ (**1**), the first compound with a discrete $Fe^{III}{}_4(\mu_4\text{-}O)$ unit, offered the unique opportunity to characterize in depth the magnetic properties of a $Fe_4(\mu_4\text{-}O)$ core that is present in many high-nuclearity clusters. Combined magnetic susceptibility and Mössbauer spectroscopic studies have shown that the properties of the core are dictated by the central bridging oxido ligand, the peripheral methoxido bridges playing only a minor role. As a consequence, at low temperatures, the tetranuclear cluster can be described as the sum of two identical and symmetric dinuclear high-spin Fe(III) units that are moderately antiferromagnetically coupled through the μ_4-oxido bridge. In addition, each Fe(III) ion of a pair interacts weakly with the two sites of the second pair through the μ_4-oxido-μ-methoxido bridging pattern. This analysis is based on the respective strengths of the diagonal and vicinal magnetic-exchange interactions that are strongly dependent on the values of the Fe-(μ_4-O)-Fe angles. It can be anticipated that a stronger tetrahedral distortion will lower the weight of the diagonal interaction and therefore modify the overall magnetic properties of the cluster. The knowledge gained in the present study will undoubtedly find an application in the rational design of high-nuclearity clusters possessing interesting magnetic properties.

Acknowledgment. Coordination by the FP6 Network of Excellence "Magmanet" (contract no. 515767) is kindly acknowledged. M.M. thanks the Department of Science and Technology, New Delhi, India (Grant SR/BY/C-10/2006) for BOYSCAST Fellowship (2006−2007).

Supporting Information Available: Crystallographic data for **1** in CIF format. Figure S1 illustrates the distortion of the coordinated ligand **bisi** in the $Fe_4(\mu_4\text{-}O)$ core, and Figure S2 shows the crystal packing of $[H_3NCH_2CH_2NH_3]_2[Fe_4O(PO_4)_4] \cdot H_2O$ (CSD refcode SINVAM). CSD refcodes (with the corresponding references) for the molecular structures deposited in the CSD exhibiting the $Fe_4(\mu_4\text{-}O)$ core (Table S1). Figures S3−S10 display the Fe_n cores found in the CSD that contain the $Fe_4(\mu_4\text{-}O)$ motif. The detailed analysis of the mass-magnetic susceptibility (massic susceptibility) of compound **1** is described (Figure S11). The full spin ladder associated with two non-interacting dinuclear species with antiferromagnetically coupled $S_i = 5/2$ local spins is shown in Scheme S1. The zero-field Mössbauer spectra of **1** recorded at 4.2 and 25 K are superimposed in Figure S12. Experimental Mössbauer spectra recorded at 4.2, 25, 35, and 50 K under a 7 T external magnetic field parallel to the γ-beam are depicted in Figure S13, along with their simulations calculated for a symmetric dihigh-spin-Fe(III) system. This material is available free of charge via the Internet at http://pubs.acs.org.

(86) Powell, G. W.; Lancashire, H. N.; Brechin, E. K.; Collison, D.; Heath, S. L.; Mallah, T.; Wernsdorfer, W. *Angew. Chem., Int. Ed.* **2004**, *43*, 5772–5775.

(87) Micklitz, W.; McKee, V.; Rardin, R. L.; Pence, L. E.; Papaefthymiou, G. C.; Bott, S. G.; Lippard, S. J. *J. Am. Chem. Soc.* **1994**, *116*, 8061–8069.

(88) Foguet-Albiol, D.; Abboud, K. A.; Christou, G. *Chem. Commun.* **2005**, 4282–4284.